Available online at www.sciencedirect.com

SciVerse ScienceDirect

Procedia CIRP 8 (2013) 540 – 545

www.elsevier.com/locate/procedia

14th CIRP Conference on Modeling of Machining Operations (CIRP CMMO)

Numerical Simulation of Machining Nickel-Based Alloys

Antonio Del Prete[a,]*, Luigino Filice[b], Domenico Umbrello[b]

[a]University of Salento, Department of Engineering Innovation, Via per Monteroni, 73100 Lecce (LE), Italy
[b]University of Calabria, Department of Mechanical, Energy and Management Engineering, Ponte P. Bucci, 45C, 87036 Rende (CS), Italy
* Corresponding author. Tel.: +39-0832-297809; fax: +39-0832-297825. *E-mail address*: antonio.delprete@unisalento.it,

Abstract

The phenomenological models for material flow stress and fracture, typically used in the Finite Element simulations of machining Nickel-based alloys, are often deemed to represent only certain metallurgical material states. In contrast, these models are not suitable to describe the constitutive behavior of the workpiece for different metallurgical states (i.e., annealed, aged, etc.) and, consequently, different hardness values.
Since the description of the material behavior requires correct formulation of the constitutive law, new flow stress models which include also the hardness effect should be developed and used, for computer simulation of machining Nickel-based alloys.
This paper describes the development of a hardness-based flow stress and fracture models for machining *Inconel 718* alloy which can be applied for a wide range of work material hardness. These models have been implemented in a non-isothermal viscoplastic numerical model to simulate the influence of work material hardness on the chip formation process. The predicted results are being validated with experimental results properly carried out for this research. They are found to satisfactory predict the cutting forces, the temperature and the chip morphology from continuous to segmented chip as the hardness values change.

© 2013 The Authors. Published by Elsevier B.V. Open access under CC BY-NC-ND license.
Selection and peer-review under responsibility of The International Scientific Committee of the "14th CIRP Conference on Modeling of Machining Operations" in the person of the Conference Chair Prof. Luca Settineri

Keywords: *Machining, Inconel 718, Material characterization, FEM.*

1. Introduction

Nickel-based superalloys were created in the 1940's primarily for gas turbine application due to their long-time strength and toughness at high temperature and more creep resistance property than available stainless austenitic steels. The principal characteristics of nickel as an alloy-base are high phase stability of face-centered cubic (fcc) nickel matrix and outstanding strength retention up to 0.7 Tm (melting point). These characteristics encourage use of nickel based superalloys in vast number of applications subjected to high temperatures. Within the commercially available nickel-base superalloys, Inconel 718 is the most frequently used for many applications: aircraft gas turbines, reciprocating engines, metal processing (e.g. hot work tools and dies), space vehicles (e.g. aerodynamically heated skins, rocket engine parts) heat treating equipment, nuclear power plants, chemical and petrochemical industries, and heat exchangers.

Because of its great economic and technical importance, a large number of researches have been carried out in order to investigate and to optimize the machining process of *Inconel 718* alloy in terms of improving quality of: the components and their surface integrity, increasing productivity and lowering cost. Several improvements in term of better understanding of machining process have been also done in the last decade thank to the heavy use of Finite Element Methodology (FEM). In fact, numerous researchers involved in this field have used FEM to predict the effect of several variables, such as: cutting forces, chip morphology, surface integrity, etc. These efforts were well recognized by several review papers proposed in the last years [1, 2]. Furthermore, great efforts were recently spent in understanding and simulating the machining process and the chip formation processes in

2212-8271 © 2013 The Authors. Published by Elsevier B.V. Open access under CC BY-NC-ND license.
Selection and peer-review under responsibility of The International Scientific Committee of the "14th CIRP Conference on Modeling of Machining Operations" in the person of the Conference Chair Prof. Luca Settineri
doi:10.1016/j.procir.2013.06.147

Inconel 718 alloy [3-5]. However, most FE modeling approaches suffer from numerical convergence in elastic-visco-plastic analysis due to the lack of reliable material models since the known flow stress equations published in literature are mainly based only on the effective strain, effective strain – rate and temperature. This may be acceptable for studying the macro process outputs when *Inconel 718* is machined but is unacceptable when micromechanical and microstructural changes such as dynamic recrystallization and phase transformation during chip formation must be investigated or when the flow stress varies with different heat treatment of the material metallurgical states (i.e., aged, annealed, forged, etc.).

Recently, Shi and Attia [6] conducted an evaluation of the constitutive laws for the metal cutting processes on *Inconel 718* alloy with the aim to improve the proposed Johnson-Cook, Zerilli-Amstrong and other models. They proposed five new constitutive law formulations and the best candidates to describe the constitutive relationship of *Inconel 718* under machining conditions were those with the use of Voce equation [7] to represent the effect of strain hardening instead of Ludwik equation [8] in the first term of Johnson-Cook model. Also Ozel et al. [5] proposed a modified Johnson-Cook equation in order to take into account the microstructural changes due to the dynamic recrystallization with satisfactory validation results. However, these new models are suitable for a given metallurgical state or nearby range, but they cannot be used to cover the wide range of metallurgical states offered by *Inconel 718* alloy. Therefore, it is very important to include the effect of the hardness in the flow stress model to reflect the influence of the different heat treatment on the selected material. In fact, successful modeling and analysis of any thermo-mechanical process are strictly related to the material model being utilized.

In this paper, a detail approach to develop a hardness based material model for machining *Inconel 718* alloy is presented. In addition, both the critical damage value (Cockcroft & Latham's criterion) and the shear factor to model friction are proposed as a function of the initial hardness, cutting speed and feed rate. An iterative procedure was also utilized for determining the global heat transfer coefficient at the tool-chip and tool-workpiece interface. Finally, the proposed constitutive law formulation was implemented in the Finite Element (FE) basis by a proper user defined routine, and it is validated by comparing the predicted results, such as cutting forces, chip morphology, and temperature, with the experimental evidences properly carried out for this research.

2. Experiments

Dry orthogonal cutting tests were conducted on Inconel 718 disks characterized by two hardness values (43.5 ± 0.8 HRC and 45.8 ± 0.5 HRC) using a MAZAK QTurn CNC turning center. In particular, a bar of 347 mm as initial diameter was gently machined in order to create several disks (Figure 1 a) characterized of a thin wall geometry (10 mm depth and 2 mm thick) spaced of 4 mm each other. Coated DNMG Sandvik tool (ISO S-DNMG150616) was selected and mounted on a Sandvik DDJNR/L tool holder (providing rake and clearance angles of -6° and 4°, respectively) as shown in Figure 1 (b). The tool holder was held in a Kistler 9257 three-component piezoelectric dynamometer for force measurements. Furthermore, a thermocouple (K-type) was embedded between the tool-holder and the tool, as shown in Figure 1 (c), for measuring the temperature during machining. This local temperature will be used to determine the temperature on the cutting tool edge by inverse numerical methodology. Disks were machined at varying of: three cutting speeds and three feed rates as illustrated in Table 1; the cutting time of each test was 80-90 sec in order to reach the mechanical and thermal steady state conditions. After machining, chips were collected, then polished to observe the morphology and the geometrical parameter (peak, valley and pitch) using a light optical microscope (1000X).

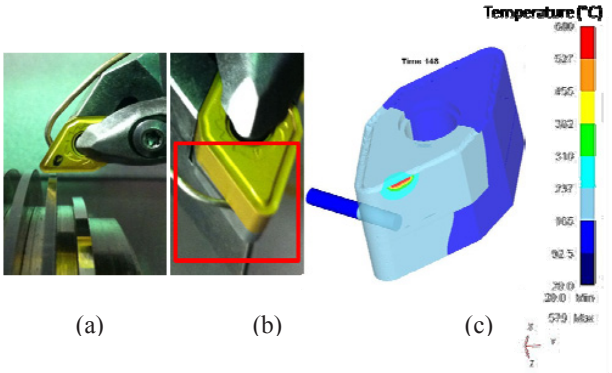

Fig. 1: (a) Scheme of the orthogonal machining and coated tool positioned for the orthogonal machining; (b) embedded thermocouple for measuring the temperature; (c) FE thermal model for inverse temperature estimation.

Table 1: Experimental machining test conditions (highlighted in grey the tests used for the FE calibration; while in white are those utilized for the FE validation)

		Cutting speed [m/min]		
		50	**60**	**70**
Feed rate [mm /rev]	**0.050**	*ID 1*	*ID 4*	*ID 7*
	0.075	*ID 2*	*ID 5*	*ID 8*
	0.100	*ID 3*	*ID 6*	*ID 9*

3. Flow Stress of *Inconel 718* Alloy at Different Hardness

3.1. Procedure

The construction of the material model to account for the influence of the workpiece hardness is considered as follows. First, a reference flow stress curve at certain workpiece hardness is chosen. Particularly, a Johnson-Cook material model for a workpiece hardness of 45 HRC (aged Inconel 718), was selected as a reference curve and given by Eq. (1).

$$\sigma_{\mathrm{Ref}} = \left(1241 + 622\varepsilon^{0.6522}\right)\left(1 + 0.0134 \cdot \ln\left(\frac{\dot{\varepsilon}}{\dot{\varepsilon}_0}\right)\right)\left(1 - \left(\frac{\mathrm{T} - 25}{1300 - 25}\right)^{1.3}\right) \quad (1)$$

The Johnson-Cook material constants were taken from research conducted by Lorentzon et al. [3], whom combined the model parameters *A*, *B*, *C*, *n* from Mitrofanov et al. [9] and *m* = 1.3. The effective plastic strain-rate, $\dot{\varepsilon}_0$, of the quasi-static test used to determine the yield and hardening parameters *A*, *B* and *n* was set as 1 s^{-1}. *T* is the workpiece temperature, and T_{melt} and T_{room} are the material melting temperature and the room temperature, respectively. Then, an additional component of stress is included to take into account the variation of the workpiece hardness on flow stress. Thus, the overall material flow stress model is presented by coupling these two parts as follows:

$$\sigma = (\varepsilon, \dot{\varepsilon}, T, HRC) = f\left(\sigma_{ref}(\varepsilon, \dot{\varepsilon}, T,), \Delta\sigma(HRC)\right) \quad (2)$$

where $\sigma_{ref}(\varepsilon, \dot{\varepsilon}, T)$ represents the flow stress curve at 45 HRC while $\Delta\sigma(HRC)$ denotes the additional component of stress, reflecting the influence of workpiece hardness.

3.2. Determination of the additional component of stress

For a given material, the hardness varies with different metallurgical states resulting in different material strength. Consequently, the initial workpiece hardness is incorporated in the flow stress using the following procedure:

1. Take yield stress and tensile strength as the start and the end points for a specific flow stress curve. If the hardness is higher, then both the yield stress and tensile strength are increased. The points within this range are obtained by assuming a linear behavior, which will be added to the reference work-hardening value.

2. For the given material assume the Young's modulus to be independent of hardness. This is the behavior shown by many materials.

This procedure was applied to the yield stress and tensile strength reported in [10] and to the ones found in this research for wokpieces at 43.5 and 45.8 HRC. Some of percentage values used to increase or decrease from 45 HRC (hardness of reference curve) to the other hardness values are shown in Table 2, while in Table 3 are reported the hardness factors determined applying a numerical procedure mentioned above (point 1). Two 2nd order polynomial functions, namely *F* and *G*, which take into account the hardness were defined by using a regression analysis on data reported in Table 3.

Table 2: Variation of the yield stress and tensile strength with the workpiece hardness.

HRC	Yield Stress [MPa]	Tensile Strength [MPa]	S_0%	S_t%
36.0	1034	1241	*-16.68%*	*-13.46%*
40.0	1096	1317	*-11.67%*	*-8.16%*
43.5	1150	1362	*-7.33%*	*-5.02%*
44.0	1179	1375	*-5.00%*	*-4.11%*
45.0	1241	1434	***Reference***	
45.8	1259	1448	*1.45%*	*0.98%*
46.0	1264	1456	*1.85%*	*1.53%*

Table 3: Hardness factors numerically determined at varying of initial workpiece hardness.

Hardness Factors			
From	**To**	**F [MPa]**	**G[MPa]**
45	46	*23.00*	*5.68*
45	45.8	*18.00*	*1.36*
45	45	*0.00*	*0.00*
45	44	*-62.00*	*-15.01*
45	43.5	*-91.00*	*-8.04*
45	40	*-144.85*	*-15.08*
45	36	*-207.00*	*-46.28*

In particular, the former, *F*, modifies the initial yield stress and the latter, *G*, the strain hardening curve.

$$\mathrm{F(HRC)} = 2.008 \cdot \mathrm{HRC}^2 - 141.97 \cdot \mathrm{HRC} + 2305.4 \quad (3)$$

$$\mathrm{G(HRC)} = -0.292 \cdot \mathrm{HRC}^2 + 28.72 \cdot \mathrm{HRC} - 700.3 \quad (4)$$

Combining Eq. (2) with Eqs. (3) and (4), the flow stress model for *Inconel 718* alloy at the different hardness can be expressed as follows:

$$\sigma_{eq} = \left(A + F + G\cdot\varepsilon + B\varepsilon^{n}\right)\left(1 + C\cdot\ln\left(\frac{\dot{\varepsilon}}{\dot{\varepsilon}_0}\right)\right)\left(1 - \left(\frac{T - T_{room}}{T_{melt} - T_{room}}\right)^{m}\right) \quad (5)$$

4. Calibration of the Proposed Constitutive Equation

4.1. Procedure

The calibration of the proposed flow stress model was carried out by FE analysis for several cutting speeds, feed rates (see Table 1) at varying of the two initial workpiece hardnesses and by comparing the predicted results with those experimentally found. In particular, the aim of this calibration phase was to determine the critical damage value (CDV) and shear factor (m) as function of the process parameters by an iterative procedure based on the error minimization. Furthermore, the same iterative procedure was also utilized for determining the global heat transfer coefficient (hint) at the tool-chip and tool-workpiece interfaces. The following assumptions are made in the FEM model: (i) rigid cutting tool; (ii) isotropic hardening for workpiece material; (iii) non – isothermal elastic – viscoplastic material governed by the incremental theory of plasticity and the Von Mises yield condition; (iv) Cockcroft & Latham's criterion [11] is employed to predict the chip segmentation.

Calibration tests and relative errors on the investigated outputs are listened in Table 4 while in Figure 2 is reported the predicted and the experimental chip morphology, including the temperature prediction, for Test ID 5 at 45.8 HRC as initial workpiece hardness.

4.2. Calibration Results

Figure 3 reports some of the calibration results regarding CDV and m as a function of initial workpiece hardness, cutting speed and feed rate. These values represent the results of the best trade-off regarding the absolute error between the investigated variables (cutting forces, chip morphology and maximum temperature on the chip). In contrast, as far as the value of hint is concerned, it was found that the constant value of 100000 kW/m^2 represents the best trade-off between the temperature prediction and the thermal stability at the tool-chip-workpiece interfaces when steady-state is reached.

Table 4: Investigated tests and relative errors obtained during the FE calibration procedure.

ID	HRC		Cutting Force [N]	Thrust Force [N]	Chip peak [µm]	Chip valley [µm]	Chip pitch [µm]	T_Max Workpiece [°C]	Damage Value (D)	Friction value (m)
2	43.5	EXP	537.5	487.1	114.8	92	50	684.00	160	0.98
		NUM	465.0	329.0	113.0	94.0	55.0	525.00		
		Err%	-13.49%	-32.46%	-1.57%	2.17%	10.00%	-23.25%		
		Ave_Err%	11.94%							
4	43.5	EXP	439.1	458.4	100.8	70.7	72.6	865.00	160	0.98
		NUM	396.0	310.0	89.7	72.5	60.4	522.00		
		Err%	-9.82%	-32.37%	-11.01%	2.55%	-16.80%	-39.65%		
		Ave_Err%	14.51%							
5	43.5	EXP	614.1	568.7	148.3	107.8	89.5	985.00	195	0.985
		NUM	481.0	325.0	128.0	101.0	84.0	570.00		
		Err%	-21.67%	-42.85%	-13.69%	-6.31%	-6.15%	-42.13%		
		Ave_Err%	18.13%							
6	43.5	EXP	665.9	496.3	189.9	122.1	112.9	962.00	240	0.98
		NUM	546.0	328.0	156.8	127.8	115.3	534.00		
		Err%	-18.01%	-33.91%	-17.43%	4.67%	2.08%	-44.49%		
		Ave_Err%	15.22%							
8	43.5	EXP	510.4	496.8	133.6	93	71.4	747.00	170	0.98
		NUM	481.0	341.0	122.0	98.0	72.0	600.00		
		Err%	-5.76%	-31.36%	-8.68%	5.38%	0.84%	-19.68%		
		Ave_Err%	10.40%							
2	45.8	EXP	658.3	510.6	94.4	66.3	62.7	737.00	120	0.9
		NUM	484.0	368.0	110.0	85.0	63.0	544.00		
		Err%	-26.48%	-27.93%	16.53%	28.21%	0.48%	-26.19%		
		Ave_Err%	19.92%							
4	45.8	EXP	472.6	422.1	87.8	64.9	50	876.00	120	0.95
		NUM	403.3	330.0	84.2	64.1	53.5	556.00		
		Err%	-14.67%	-21.82%	-4.10%	-1.23%	7.00%	-36.53%		
		Ave_Err%	9.77%							
5	45.8	EXP	657.2	560.56	141.9	98.1	87.4	990.00	220	0.97
		NUM	518.0	352.0	128.0	102.0	85.0	570.00		
		Err%	-21.18%	-37.21%	-9.80%	3.98%	-2.75%	-42.42%		
		Ave_Err%	14.98%							
6	45.8	EXP	795.6	541.5	170.9	113.5	67.8	969.00	150	0.98
		NUM	526.0	385.0	142.0	111.0	69.0	600.00		
		Err%	-33.89%	-28.90%	-16.91%	-2.20%	1.77%	-38.08%		
		Ave_Err%	16.73%							
8	45.8	EXP	627.8	488.2	136.1	89.3	74	1037.00	160	0.98
		NUM	500.0	372.0	115.8	88.3	67.0	614.00		
		Err%	-20.36%	-23.80%	-14.92%	-1.12%	-9.46%	-40.79%		
		Ave_Err%	13.93%							

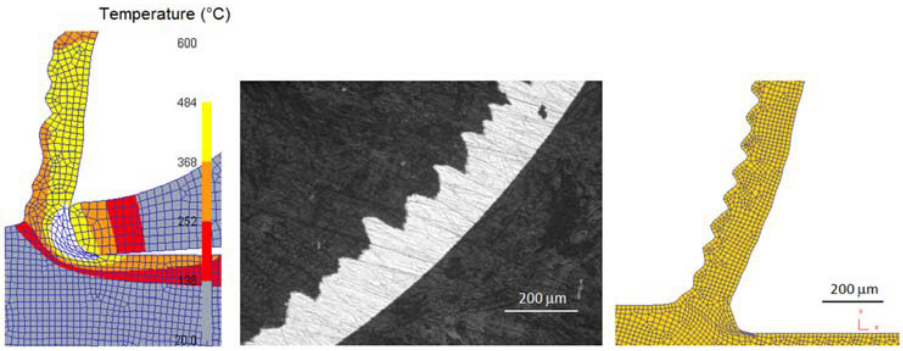

Figure 2: Temperature prediction (a) and chip geometry obtained during machining of Inconel 718 alloy (45.8 HRC) at 60 m/min and 0.075 mm/rev: (b) experimental; (c) numerical.

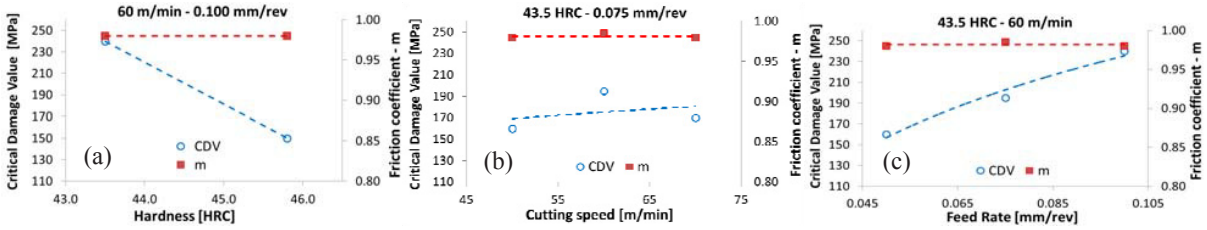

Figure 3: Influence of initial workpiece hardness and cutting process parameters on CDV and m: (a) workpiece hardness; (b) cutting speed; (c) feed rate.

Table 5: Investigated tests and relative errors obtained during the FE validation phase.

ID	HRC	Damage Value (D)	Friction value (m)		Cutting Force [N]	Thrust Force [N]	Chip peak [µm]	Chip valley [µm]	Chip pitch [µm]	T_Ave Tool [°C]
1	43.5	227.7	0.947	EXP	505.3	482.7	139.1	96.8	77.4	554.00
				NUM	440.0	320.0	105.0	86.0	91.0	560.00
				Err%	-12.92%	-33.71%	-24.51%	-11.16%	17.57%	1.08%
				Ave_Err%	16.83%					
3	43.5	208.2	0.96	EXP	748.9	615.1	179.3	132.4	79.2	630.00
				NUM	647.2	443.4	159.4	121.4	91.7	653.35
				Err%	-13.58%	-27.91%	-11.09%	-8.31%	15.78%	3.71%
				Ave_Err%	13.40%					
7	43.5	209.7	0.9	EXP	453	483.5	125.8	88.5	61.4	657.00
				NUM	411.4	339.4	114.5	80.2	77.0	639.44
				Err%	-9.18%	-29.80%	-8.98%	-9.38%	25.41%	-2.67%
				Ave_Err%	14.24%					
9	43.5	214	0.977	EXP	653.1	488	172.9	124.9	85.1	705.00
				NUM	585.2	387.8	151.7	117.1	93.2	692.07
				Err%	-10.40%	-20.53%	-12.26%	-6.24%	9.48%	-1.83%
				Ave_Err%	10.12%					
1	45.8	134.7	0.929	EXP	464.6	423.8	129.8	94.2	67.4	618.00
				NUM	456.0	384.0	92.0	65.8	75.0	590.00
				Err%	-1.85%	-9.39%	-29.12%	-30.15%	11.28%	-4.53%
				Ave_Err%	14.39%					
3	45.8	161	0.935	EXP	804.5	529.5	177.9	136.3	79.3	670.00
				NUM	712.0	442.3	156.0	112.3	84.0	604.00
				Err%	-11.50%	-16.47%	-12.31%	-17.61%	5.93%	-9.85%
				Ave_Err%	12.28%					
7	45.8	153.5	0.921	EXP	470	420.6	117.2	82.6	50.4	702.00
				NUM	407.4	318.3	105.7	75.5	59.2	603.40
				Err%	-13.31%	-24.32%	-9.79%	-8.64%	17.38%	-14.05%
				Ave_Err%	14.58%					
9	45.8	172	0.978	EXP	781.1	540.3	169.2	120	98.2	760.00
				NUM	640.3	466.6	145.3	109.4	85.2	713.43
				Err%	-18.03%	-13.64%	-14.13%	-8.83%	-13.24%	-6.13%
				Ave_Err%	12.33%					

The variation of the CDV and m with the workpiece hardness is shown in Figure 3 (a). It can be noted that different CDV are found for different hardness, because its change for the same material causes the change of material flow stress, thus segmentation of the chip. This curve also confirms that as hardness increases, the fracture toughness (or the critical damage value) decreases. Concerning the friction factor, its tendency is to remain almost constant with the increasing of the workpiece hardness. It can be also noted as lower *CDV* values are found to increase when both the process parameters increase since their rise produces an

increasing of the temperature and, consequently, an higher thermal softening phenomenon (i.e., generation of an higher shear localized deformation area. Finally, the friction factor in general slightly increases or remains constant with the increasing of both the process parameters (Figure 3).

5. FE Validation

5.1. Procedure

The validation of the proposed flow stress model was executed for the other tests, which were not used in the FE calibration (Table 1).

However, before starting with the FE validation, a flow stress correction was necessary since during the FE calibration, the errors on principal cutting force were, in some cases, higher than 20%. Therefore, a modification of parameter *F,* as reported in Eqs. (6) and (7), has been needed for improving the predictiveness of the proposed flow stress models. These corrections have been done taking into account the discrepancy on principal cutting force prediction and the compression test results carried out on samples at 43.5 and 45.8 HRC.

$$\sigma_{eq} = \left(A + (F + 200) + G \cdot \varepsilon + B\varepsilon^{n}\right)\left(1 + C \cdot \ln\left(\frac{\dot{\varepsilon}}{\dot{\varepsilon}_0}\right)\right)\left(1 - \left(\frac{T - T_{room}}{T_{melt} - T_{room}}\right)^{m}\right) \quad (6)$$

$$\sigma_{eq} = \left(A + (F + 265) + G \cdot \varepsilon + B\varepsilon^{n}\right)\left(1 + C \cdot \ln\left(\frac{\dot{\varepsilon}}{\dot{\varepsilon}_0}\right)\right)\left(1 - \left(\frac{T - T_{room}}{T_{melt} - T_{room}}\right)^{m}\right) \quad (7)$$

Validation tests and relative errors on the investigated outputs are shown in Table 5 while in Figure 4 is reported the predicted and the experimental chip morphology for Test *ID 9* at 43.5 HRC as initial workpiece hardness.

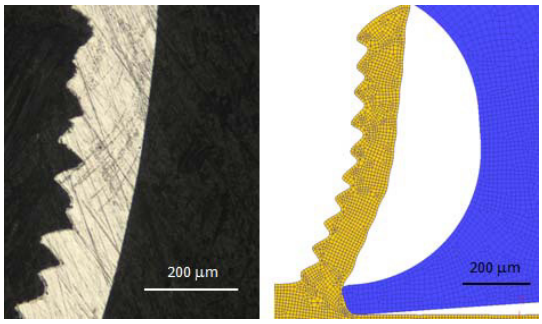

Fig. 4: Chip geometry obtained during machining of Inconel 718 alloy (43.5 HRC) at 70 m/min and 0.1 mm/rev: (b) experimental; (c) numerical.

6. Conclusions

In this paper, a hardness-based flow stress model for Inconel 718 alloy was developed. Moreover, both the critical damage and friction factor values were defined as a function of the material hardness, cutting speed and feed rate. Based on these results it can be concluded that the present FE model which incorporate the proposed flow stress can be applied to simulate the machining process of Inconel 718 alloy and to reproduce some characteristic features of the chip formation process for different metallurgical states (aged, forged, annealed, etc.).

Acknowledgements

The authors gratefully thank Dr. Serafino Caruso for his contribution in developing this study.

References

[1] Guo, Y.B., Li, W., Jawahir, I.S., 2009, Surface Integrity Characterization and Prediction in Machining of Hardened and Difficult to Machine Alloys: a State-of-Art Research Review and Analysis, Mach. Sci. Technol., 13:437-470.

[2] Ulutan, D., Özel, T., 2011, Machining induced surface integrity in titanium and nickel alloys: A review, Int. J. Mach. Tools & Manuf., 51:2250-2280.

[3] Lorentzon, J., Järvstråt, N., Josefson, B.L., 2009, Modelling chip formation of alloy 718, J. Mater. Proc. Technol., 209:4645-4653.

[4] Calamaz, M., Coupard, D., Girot, F., 2008, A new material model for 2D numerical simulation of serrated chip formation when machining titanium alloy Ti-6Al-4V, Int. J. Mach. Tools & Manuf., 48:275-288.

[5] Ozel, T., Llanos, I., Soriano, J., Arrazola, P.J., 2011, 3D finite Element Modelling of chip Formation Process for Machining Inconel 718: Comparison of FE Predictions, Mach. Sci. Technol. 15/1:21-46.

[6] Shi, B., Attia, M.H., 2010, Evaluation criteria of the constitutive law formulation for the metal-cutting process, Proc. IMechE Part B: J. Eng. Manuf., 224:1313-1328.

[7] Voce, E., 1948. The relationship between stress and strain for homogeneous deformation. J. Inst. Metals, 74: 537-562.

[8] Ludwik, P., 1909, Elemente der technologischen mechanik. 32–38 (Julius, Springer, Berlin).

[9] Mitrofanov, A.V., Babitsky, V.I., Silberschmidt, V.V., 2005, Thermomechanical finite element simulations of ultrasonically assisted turning. Computational Mater. Sci. 32/3-4:463–471.

[10] Special Metals Corporation, 2007, INCONEL Alloy 718. Publication Number SMC-045: 1-28.

[11] Cockroft, M.G., Latham, D.J., 1968, Ductility and Workability of Metals. J. Inst. Metals, 96: 33-39.